

GYROTRON PERFORMANCE ON THE 110 GHz INSTALLATION AT THE DIII-D TOKAMAK

by
I. GORELOV, J.M. LOHR, D. PONCE, R.W. CALLIS,
H. IKEZI, R.A. LEGG, AND S.E. TSIMRING*

This is a preprint of a paper to be presented at the
24th International Conference on Infrared and
Millimeter Waves, September 5-10, 1999, Monterey,
California and to be published in the *Proceedings*.

*Private Consultant

Work supported by
the U.S. Department of Energy
under Contract No. DE-AC03-99ER54463

GA PROJECT 30033
JUNE 1999



DISCLAIMER

This report was prepared as an account of work sponsored by an agency of the United States Government. Neither the United States Government nor any agency thereof, nor any of their employees, make any warranty, express or implied, or assumes any legal liability or responsibility for the accuracy, completeness, or usefulness of any information, apparatus, product, or process disclosed, or represents that its use would not infringe privately owned rights. Reference herein to any specific commercial product, process, or service by trade name, trademark, manufacturer, or otherwise does not necessarily constitute or imply its endorsement, recommendation, or favoring by the United States Government or any agency thereof. The views and opinions of authors expressed herein do not necessarily state or reflect those of the United States Government or any agency thereof.

DISCLAIMER

Portions of this document may be illegible in electronic image products. Images are produced from the best available original document.

Gyrotron Performance on the 110 GHz Installation at the DIII-D Tokamak

I. Gorelov, J.M. Lohr, D. Ponce, R.W. Callis, H. Ikezi, R.A. Legg and S.E. Tsimring*

General Atomics, P.O. Box 85608, San Diego CA 92186-5608

*S.E. Tsimring Private Consultant

Abstract

The 110 GHz gyrotron system on the DIII-D tokamak comprises three different gyrotrons in the 1 MW class. The individual gyrotron characteristics and the operational experience with the system are described.

Gyrotron Characteristics

The gyrotrons are of two general types, characterized by either a diode or triode magnetron injection gun (MIG) and are further differentiated by the power handling capability of their output windows which, in turn, determines the designed characteristics of the output rf beams. The typical best performance for the devices is summarized in Table 1.

Table 1. Gyrotron typical best performance

Manufacturer	Gun Type	Window	Achieved Performance	RF Beam	Manufacturer's Type, Local Name
Gycom	Diode BN MIG	BN	0.8 MW 2.0 s	Spread	Centaur, Katya [1]
CPI	Triode Sapphire MIG	Sapphire	1.1 MW 0.6 s	Spread	8011A, Dorothy [2]
CPI	Triode Diamond MIG	Diamond	0.5 MW 4.2 s	Gaussian	8110, Toto [3]

Measurements of the rf output power are made using calorimetry on the window cooling circuits. The BN window on Katya is edge cooled by water and has 3.7% absorption. The sapphire window on Dorothy is a face-cooled double disk with a chlorofluorocarbon, FC-75, as the coolant. This window has 1.7% absorption. The window on Toto is a diamond disk. For this window, the absorption is too low for reliable calorimetric measurements so output power was measured directly using a black planar load with 1,octanol as the working fluid. Octanol has linear absorption of 13 dB per cm traversed [4] and the load has a minimum thickness of 2.5 cm. The output powers and rf generation efficiencies for each of the gyrotrons are presented in Fig. 1.

The diode gyrotron has demonstrated somewhat better efficiency than either of the triode tubes. The triode tube, Dorothy, produced the highest output power, 1.09 MW averaged over a 600 ms pulse, but the triode tube with the diamond output window has consistently had low rf efficiency, averaging 20%–25% in

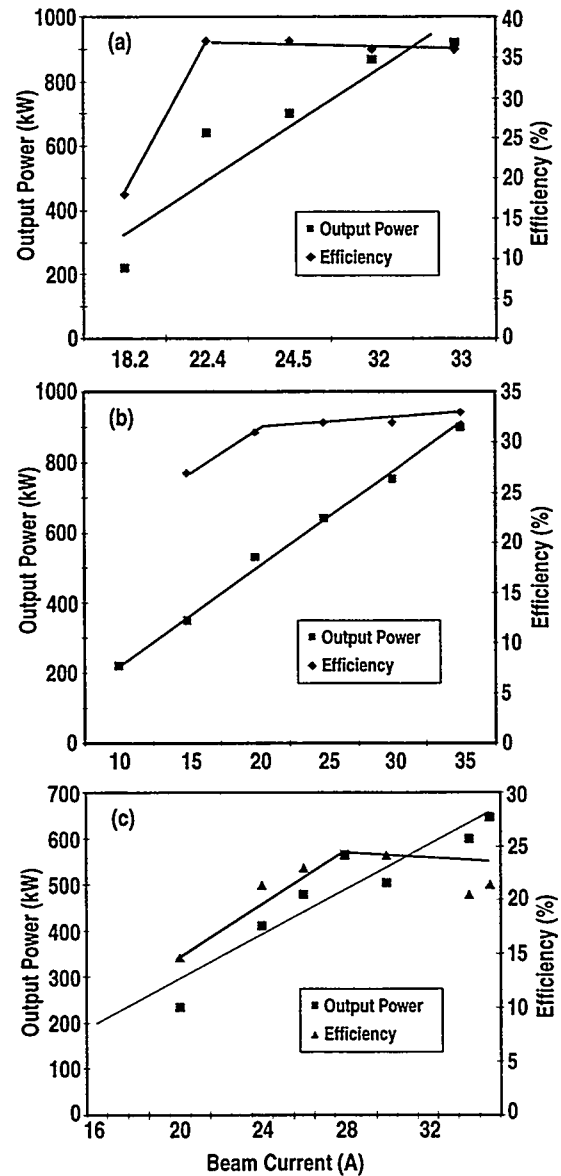


Figure 1. (a) The rf output power and efficiency for Katya as a function of the electron beam current. (b) The rf output power and efficiency for Dorothy as a function of the electron beam current. The efficiency is calculated from $P_{rf}/I_b V_b$ and the rf power is measured calorimetrically from the window cooling/circuit or directly with the planar load either for long (typically 500 ms) single pulses or for equilibrium conditions with short (typically 5 ms at 1 Hz) pulses at fixed repetition frequency. The calorimetry is calibrated from the response to resistive heaters delivering a known energy to the cooling fluid. (c) The rf output power and efficiency for Toto as a function of the electron beam current.

measurements at DIII-D. In initial tests of this gyrotron at CPI, a higher efficiency of about 30% was measured. The reason for the discrepancy is under investigation.

RF Beam Profiles

For both the BN and sapphire windows, the central power density of a pure Gaussian beam would exceed the capabilities of the windows; therefore, higher order modes are mixed internally with the Gaussian beam to spread the output power over a larger area and decrease the peak density. The diamond window, with its extremely low absorbed power, can tolerate a Gaussian beam and Toto was designed to produce such a beam. Infrared camera measurements of the power profiles of the rf beams propagating from the three gyrotrons are shown for various distances from the gyrotron windows in Figs. 2, 3 and 4. The profiles were taken under different conditions and the size scaling is not preserved exactly in the figures, however, the total field

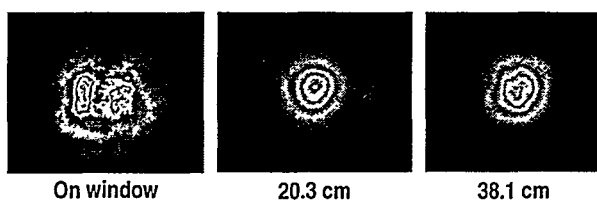


Figure 2. Infrared measurements of the beam from the diode gyrotron, Katya, as a function of distance from the BN output window.

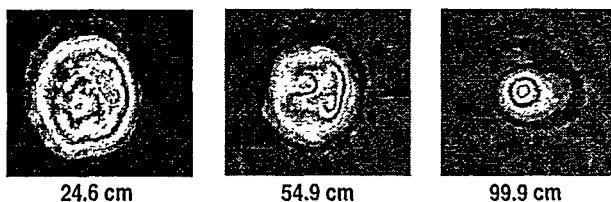


Figure 3. Infrared measurements of the beam from the triode gyrotron, Dorothy, as a function of distance from the sapphire output window.

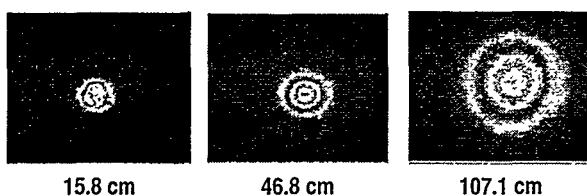


Figure 4. Infrared measurements of the beam from the triode gyrotron, Toto, as a function of distance from the diamond output window. The beam is approximately a free space Gaussian.

of view is about 12 cm horizontally and the camera dynamic range is 25 dB.

After the rf exits the gyrotron, it is reflected from a pair of mirrors designed to perform phase correction [5] and focus the beam to a Gaussian waist at the input to the corrugated circular waveguide line. The efficiency of coupling to the guide is about 83%, that is, calorimetrically measured losses in the mirror box are about 17% for all three gyrotrons. The transmission line is about 96% efficient, therefore, more than 75% of the rf power which passes through the gyrotron windows is delivered to the tokamak through about 40 m of waveguide. The transmission system is evacuated.

Parasitic Emission

Regardless of the type of electron gun, the electron beam is compressed after leaving the cathode by an increasing magnetic field prior to propagation through the cavity. Only electron perpendicular energy couples to the cavity modes. The electron pitch angle, v_{\perp}/v_{\parallel} , which is controlled by a combination of gun parameters and an externally applied magnetic field bucking the main magnetic field at the gun, cannot be increased arbitrarily, however, without reflecting the electrons from the magnetic mirror field at the cavity.

Reflected electrons can be accumulated between the cavity and the gun, sloshing with a frequency corresponding to the round trip transit time. If reflected electrons strike the cathode structure with energy greater than about 100 eV, secondary electrons can be emitted, which can rapidly increase the cathode current. If an undesired part of the cathode structure is heated by reflected electrons and begins to emit, the cathode current can also increase, but with a thermal time constant of several seconds.

Both types of behavior have been observed. The slow, thermal increase in beam current is characteristic of the diode tube, Katya, and the rapid increase due to secondary emission is typical for the triode gyrotron, Toto. In Figs. 5 and 6, the parasitic emission from Katya and Toto are shown.

The Dorothy gyrotron, the best performer from the standpoint of output power, appears to be free from parasitic emission.

The frequency of the sloshing electrons for the gyrotrons at DIII-D, estimated from the gyrotron geometries and the electron beam energies, is approximately 100 MHz, consistent with the spectra observed.

On Katya, there is a beam current threshold for parasite emission. At low currents, near 4.0A, the parasite frequency is not well established and bursts near 100 MHz are seen. As the current is increased, emission becomes continuous but emission from 95 to 105 MHz. For higher currents, the spectrum becomes more narrow and the sidebands disappear

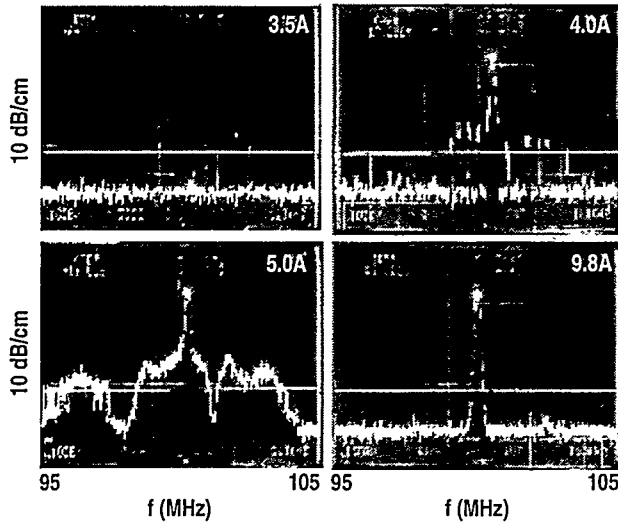


Figure 5. Parasitic emission spectra for Katya near 100 MHz. The parasite has a threshold in beam current of about 4A as seen in the top two figures for 3.5 and 4.0A. The lower two spectra are for $I_b = 5.0$ and 33.0A and show how the fully developed instability has a very narrow and rather monochromatic spectrum.

leaving a single, nearly monochromatic 96 MHz parasite for 33.0A, the gyrotron operating current.

It is important to note that the parasitic emission does not necessarily result in an appreciable decrease in the rf output power, therefore, it must involve only a small number of electrons which do not seriously corrupt the electron beam. But the gyrotron operating point can be changed and ancillary electronics can be adversely affected when the parasite is generated.

Conclusions

The performance of the three gyrotrons installed on the DIII-D tokamak shows that the electron beam dynamics and high power rf generation at 110 GHz are well enough understood and that these devices can be considered to represent mature technology which is ready for applications. Additional development will improve the understanding of such effects as reflected electrons and low frequency parasitic emission which could be important at the

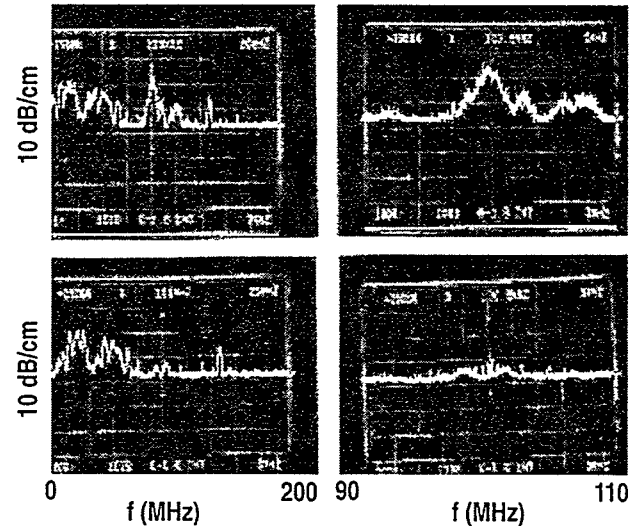


Figure 6. Parasitic emission spectra for Toto near 100 MHz. The Toto spectrum amplitude is much lower than Katya's. The total emission from Katya is estimated at several kilowatts, but the Toto amplitude is comparable to other signals in the broadcast bands on an antenna near the gyrotron. The upper two traces are with the gyrotron operating, the lower two are without gyrotron operation.

longer pulse lengths made possible by low loss diamond output windows.

Acknowledgements

This is a report of work supported by the U.S. Department of Energy under Contract No. DE-AC03-99ER54463.

References

- [1] V.E. Myasnikov *et al.*, Proc. 22nd Int. Conf. on Infrared and Millimeter Waves (1997) p. 102.
- [2] K. Felch *et al.*, IEEE Transactions on Plasma Science 24, 558 (1996).
- [3] K. Felch *et al.*, Proc. 23rd Int. Conf. on Infrared and Millimeter Waves (1998) p. 367.
- [4] H. Stickle, Int J. Electronics 64, 63 (1988).
- [5] A.V. Chirkov *et al.*, Opt. Commun. 115, 449 (1995); D.R. Denison *et al.*, Proc. 23rd Int. Conf. on Infrared and Millimeter Waves (1998) p. 119.